

Investigation of structure and morphology of Cu-Mn-Zr-Ce-O solid solutions

I. V. Zagaynov^{1,†}, A. A. Konovalov¹, E. A. Koneva²

[†]igorscience@gmail.com

¹A.A. Baikov Institute of Metallurgy and Materials Science, 49 Leninskii ave., Moscow, 119334, Russia

²D. Mendeleev University of Chemical Technology of Russia, 9 Miusskaya sq., Moscow, 125047, Russia

Materials based on ceria are of interest due to the fact that they have a large oxygen storage capacity and high mobility of oxygen, which can offer high catalytic activity and electrical conductivity. It is well known that the copper or manganese doping of ceria leads to a synergistic effect — a decrease in temperature of the catalytic reaction and the activation energy, but, unfortunately, the solid solutions Cu-Mn-(Zr)-Ce-O could not be presented earlier. So, a series of Cu-Mn-Zr-Ce-O solid solutions was synthesized by co-precipitation method with sonication. The crystallite size of all samples is about 7–9 nm, and does not depend on the Cu/Mn ratio. The variation in the lattice parameter corresponds to the Vegard's law and can be described by the semiempirical equation for ceria based solid solutions: Cu-Mn-Ce-O is clear correlated to the equation, but Cu-Mn-Zr-Ce-O is not. Pore size distributions in the range of 2–25 nm for Cu-Mn-Ce-O systems and 2–40 nm for Cu-Mn-Zr-Ce-O systems were observed. Thereby the preparing of homogeneous solid solutions gives the better textural property, thermal stability, catalytic and other properties as compared to domain- or phase-segregated nonhomogeneous ones. Therefore, this method allowed creating such homogeneous solid solutions, giving the better properties for their application. These systems can be applied in catalysis as a support or in IT-SOFC as an electrolyte.

Keywords: ceria, solid solution, mesopores, nanoparticle.

УДК: 546.05

Изучение структуры и морфологии твердых растворов Cu-Mn-Zr-Ce-O

Загайнов И. В.^{1,†}, Коновалов А. А.¹, Конева Е. А.²

¹Институт металлургии и материаловедения имени А. А. Байкова РАН, Ленинский пр., 49, Москва, 119334, Россия

²Российский химико-технологический университет им. Д. И. Менделеева, Миусская пл. 9, Москва, 125047, Россия

Материалы на основе диоксида церия представляют интерес в связи с тем, что они обладают большим запасом кислорода и его высокой подвижностью, в свою очередь это может обеспечить высокую каталитическую активность и электропроводность. Хорошо известно, что допирование диоксида церия медью или марганцем приводит к синергетическому эффекту — снижению температуры каталитической реакции и энергии активации процесса, однако, твердые растворы Cu-Mn-(Zr)-Ce-O не были представлены ранее в литературе. Таким образом, серия таких твердых растворов была синтезирована методом соосаждения с одновременным использованием ультразвуковой обработки. Размер кристаллитов всех образцов составлял около 7–9 нм и не зависел от отношения Cu/Mn. Изменение параметра кристаллической решетки соответствует закону Вегарда и может быть описано полуэмпирическим уравнением для твердых растворов на основе диоксида церия: система Cu-Mn-Ce-O хорошо коррелирует с уравнением, а система Cu-Mn-Zr-Ce-O нет. Распределение пор по размерам было в диапазоне 2–25 нм для материала Cu-Mn-Ce-O и 2–40 нм для материала Cu-Mn-Zr-Ce-O. Таким образом, получение гомогенных твердых растворов даст лучшие текстурные свойства, термическую стабильность, каталитические свойства, электропроводность и другие преимущества, по сравнению с неоднородными с включением и сегрегированием других фаз или доменных структур. Поэтому предложенный подход позволил создать такие материалы с улучшенными характеристиками для их дальнейшего применения. Эти системы могут быть использованы в качестве носителей катализаторов или электролита среднетемпературных твердооксидных топливных элементов.

Ключевые слова: диоксид церия, твердый раствор, мезопоры, наночастицы.

1. Introduction

Materials based on ceria are of interest due to the fact that they have a large oxygen storage capacity (OSC) and high mobility of oxygen, which can offer high catalytic activity and electrical conductivity. Thus, for the effective implementation of the process the crystal structure with a sufficiently high oxygen vacancy defect concentration is required. The reason is the oxygen donation of ceria caused by partial $\text{Ce}^{4+}/\text{Ce}^{3+}$ reduction on the particle surface.

It is well known that the copper or manganese doping of ceria leads to a synergistic effect — a decrease in temperature of the catalytic reaction and the activation energy, but, unfortunately, the solid solutions Cu-Mn-(Zr)-Ce-O could not be presented earlier. For example, copper or manganese is deposited by impregnation method, resulting in Cu-CeO₂ or Mn-CeO₂, respectively, but no uniform solid solution was obtained, and an additional phase was [1–4]. The only article, where the authors attempted to obtain solid solutions Cu-Mn-Ce-O (Cu/Mn=1, Cu+Mn/Ce=3:17; 3:7; 4:6) by hydrothermal method, was published [5], but the system was studied by XRD to be concluded on the formation of a solid solution, but according to the XPS data metal content of copper and manganese in the surface layer was significant, but it is known that the solubility of Mn or Cu in the ceria lattice is less than 10 mol.%, so its single phase catalyst for organic compound oxidation ($\text{Cu}_{0.15}\text{Mn}_{0.15}\text{Ce}_{0.7}\text{O}_2$) is to doubt.

It is known that the sonochemical method [6, 7] has been proved to be useful method to obtain solid solutions and provide optimizing the phase, composition and morphology of nanoparticles. Ultrasonic waves radiate through the precursor solution. It causes alternating high-low pressure in the solution and leads to the formation, growth, and implosive collapse of bubbles in the reaction mixture. The collapse of bubbles with short lifetime produces intense local heating. According to the hot spot theory, very high temperatures (>5000°C) and pressures of roughly 1000 atm are obtained upon the collapse of a bubble, so these critical conditions provide the enough energy for the formation of the certain phase. In this work, Cu-Mn-Zr-Ce-O solid solutions were synthesized by co-precipitation method with sonication, and structural and morphological properties were studied.

2. Material and methods

$\text{Ce}(\text{NO}_3)_3 \cdot 6\text{H}_2\text{O}$, $\text{ZrO}(\text{NO}_3)_2 \cdot 7\text{H}_2\text{O}$, $\text{Cu}(\text{NO}_3)_2 \cdot 3\text{H}_2\text{O}$, $\text{Mn}(\text{NO}_3)_2 \cdot 4\text{H}_2\text{O}$ (Acros Organics) were used as metal precursors. Appropriate amounts of salts were dissolved in concentrated nitric acid (68%) with the concentration of salts of 0.667 M. After dissolution of salts, this mixture was added to distillate water, giving concentration of 0.1 M. Then, the co-precipitation was carried out by the addition of 2.5 M KOH solution up to pH 11. Ultrasonic processing (35 kHz, 150 W) was used during all process at 30°C under stirring. The resulting precipitates were filtered, washed with distilled water-ethanol solution ($\text{H}_2\text{O}/\text{C}_2\text{H}_5\text{OH}=9$ vol.), dried at 150°C for 12 h, and calcined in static air by heating at a rate of 4°C/min from room temperature to 500°C and kept at 500°C for 1 h in the muffle furnace.

All powders were characterized by XRD (Rigaku MiniFlex 600, CuK α radiation); particle size (d_{XRD}) measurements were made by applying the Scherrer equation to the full-width at half maximum after accounting for instrumental broadening using germanium as reference; d_{XRD} was calculated not on a separate peak, but was on all planes during the fitting of the spectrum; quantitative phase analysis was calculated by the Rietveld method. Nitrogen adsorption-desorption method (TriStar 3000 Micromeritics), TEM (Omega Leo-912AB), TG-DSC (Netzsch STA449F3) were also used.

3. Results and discussion

The XRD patterns of the samples are shown in Fig. 1a. All samples present the characteristic peaks of pure cubic fluorite structure of ceria (JCPDS-34-0394), and no other phases (diffraction peaks) of MnO_x, CuO_x, and CuMnO_x were detected (Fig. 1b), indicating the fine dispersion of dopants and formation of Cu-Mn-(Zr)-Ce-O solid solution. It is known that the solubility limit of Mn and Cu in ceria is

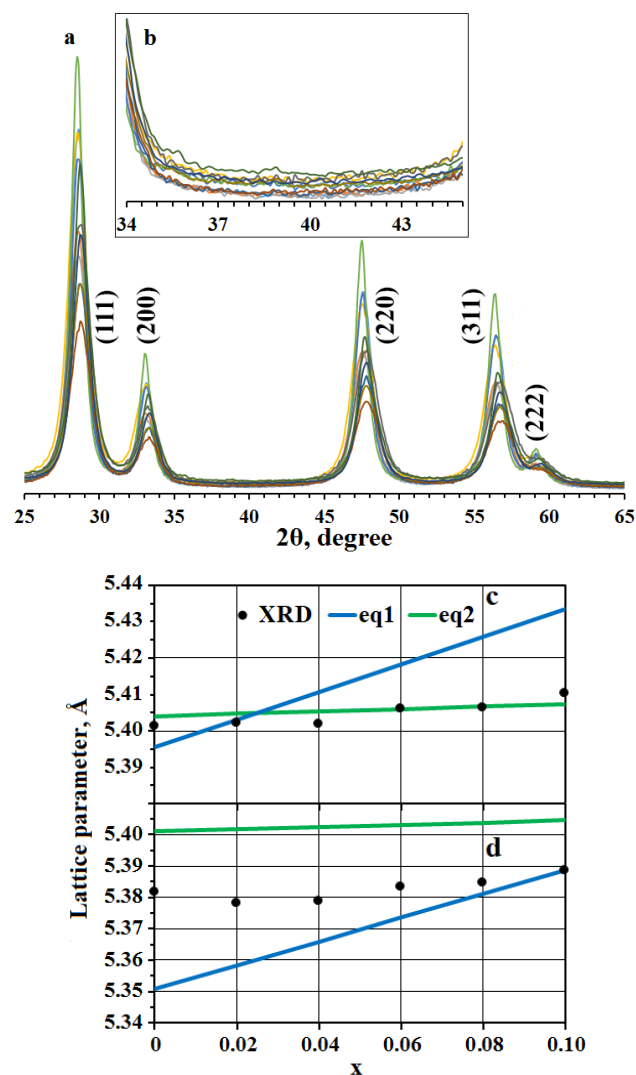


Fig. 1. (Color online) XRD patterns of powders with CuK α radiation (a), delineated area (b) — no additional Cu-O or Mn-O phases; the change in the lattice parameter in $\text{Cu}_x\text{Mn}_{0.1-x}\text{Ce}_{0.9}\text{O}_2$ (c) or $\text{Cu}_x\text{Mn}_{0.1-x}\text{Zr}_{0.1}\text{Ce}_{0.8}\text{O}_2$ (d) systems.

less than 10 mol.% and highly depends on the preparation procedure [8, 9]. The crystallite size and lattice parameter of solid solutions are presented in Table 1. The crystallite size of all samples is about 7–9 nm, and did not depend on the Cu/Mn ratio. According to TEM, all powders consisted of particle aggregates (Fig. 2); individual particles were about 4–9 nm, which corresponds to the crystallite size, calculated by Scherrer equation. Doping ceria induces uniform strain in the lattice because the material is elastically deformed.

This effect causes the lattice plane spacing to change and the diffraction peaks to shift to new 2θ positions. This shift is indicative of a change in the lattice parameter (Table 1, Fig. 1c and 1d). This corresponds to the increase of the cell parameter (a) with the increase of Cu/Mn ratio, and in the Zr-doped systems the lattice parameter is smaller, and all of this directly related to the ionic radii: the ionic radii of Cu^{2+} and Mn^{3+} - Mn^{4+} (because these ions dominated in solid solutions in according to previous investigations,

Table 1. Main characteristics of ceria-based powders ($\text{Cu}_x\text{Mn}_{0.1-x}\text{Ce}_{0.9}\text{O}_2$ or $\text{Cu}_x\text{Mn}_{0.1-x}\text{Zr}_{0.1}\text{Ce}_{0.8}\text{O}_2$).

No	Sample	d_{XRD} , nm	Lattice parameter, Å	S_{BET} , m^2/g	Cumulative volume of pores, cm^3/g
0	CeO_2 [10]	14	5.4094	53	0.1070
1	$\text{Cu}_0\text{Mn}_{0.1}\text{Ce}_{0.9}\text{O}_2$	9	5.4013	91	0.3185
2	$\text{Cu}_{0.02}\text{Mn}_{0.08}\text{Ce}_{0.9}\text{O}_2$	7	5.4021	84	0.2469
3	$\text{Cu}_{0.04}\text{Mn}_{0.06}\text{Ce}_{0.9}\text{O}_2$	7	5.4019	91	0.2837
4	$\text{Cu}_{0.06}\text{Mn}_{0.04}\text{Ce}_{0.9}\text{O}_2$	8	5.4061	94	0.2532
5	$\text{Cu}_{0.08}\text{Mn}_{0.02}\text{Ce}_{0.9}\text{O}_2$	9	5.4064	79	0.2127
6	$\text{Cu}_{0.1}\text{Mn}_0\text{Ce}_{0.9}\text{O}_2$	12	5.4103	55	0.1858
7	$\text{Cu}_0\text{Mn}_{0.1}\text{Zr}_{0.1}\text{Ce}_{0.8}\text{O}_2$	7	5.3816	75	0.3291
8	$\text{Cu}_{0.02}\text{Mn}_{0.08}\text{Zr}_{0.1}\text{Ce}_{0.8}\text{O}_2$	6	5.3781	67	0.1863
9	$\text{Cu}_{0.04}\text{Mn}_{0.06}\text{Zr}_{0.1}\text{Ce}_{0.8}\text{O}_2$	7	5.3788	71	0.2501
10	$\text{Cu}_{0.06}\text{Mn}_{0.04}\text{Zr}_{0.1}\text{Ce}_{0.8}\text{O}_2$	7	5.3832	36	0.1140
11	$\text{Cu}_{0.08}\text{Mn}_{0.02}\text{Zr}_{0.1}\text{Ce}_{0.8}\text{O}_2$	8	5.3845	31	0.0868
12	$\text{Cu}_{0.1}\text{Mn}_0\text{Zr}_{0.1}\text{Ce}_{0.8}\text{O}_2$	8	5.3886	40	0.1159

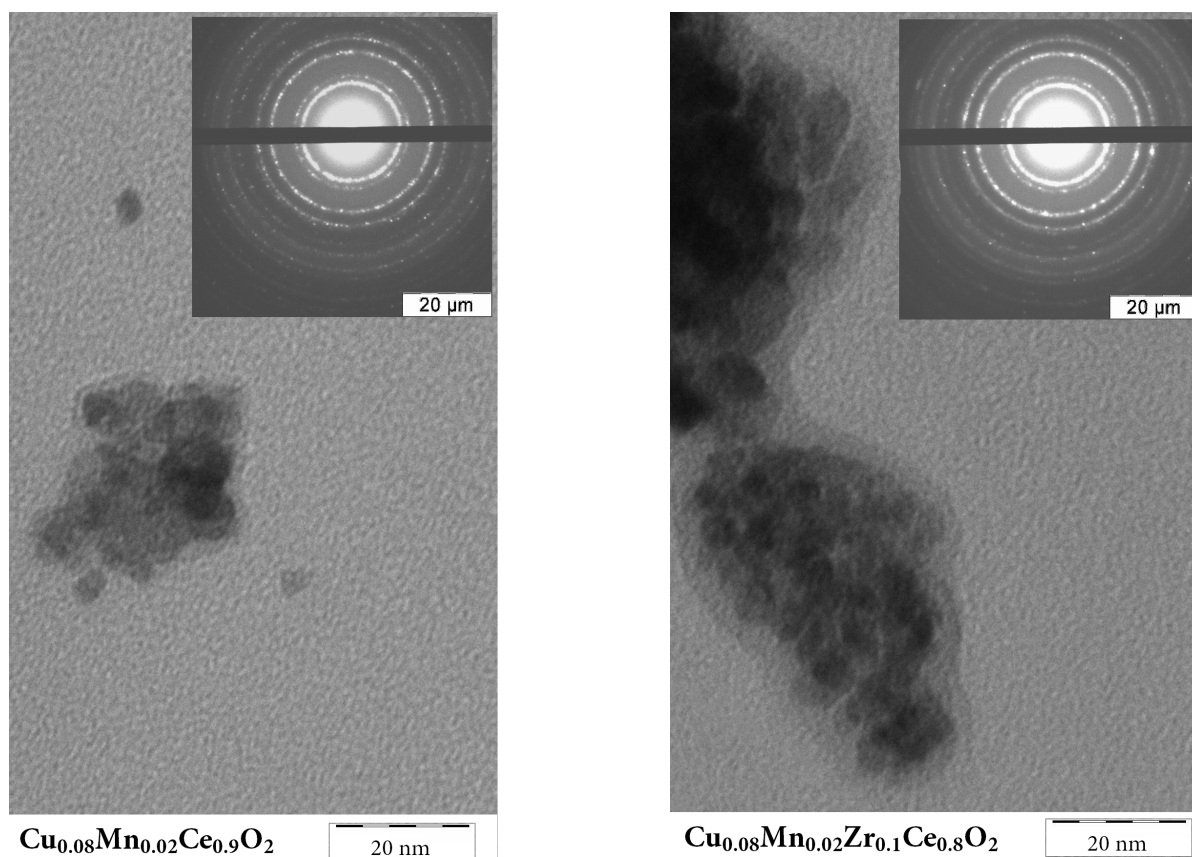


Fig. 2. TEM microphotos of obtained powders.

and may exist Cu^+ and Mn^{2+} , but their part is less than 10%, $\text{Mn}^{3+}/\text{Mn}^{4+} \sim 70/30$ are 0.73 Å, 0.58 Å, and 0.53 Å, respectively, and Zr^{4+} is 0.84 Å, which is smaller than that of Ce^{4+} (0.97 Å). Lattice parameter dependence on nominal metal content was approximately linear, i.e. corresponds to the Vegard's law. The variation in the lattice parameter (a , Å) of the fluorite cubic structure can be described by the two equations: based on the ion-packing model (equation 1) [11], or the most used semiempirical equation for ceria based solid solutions (equation 2) [12]:

$$a = 0.9971 \times \left[\frac{4}{\sqrt{3}} \times \sum_i (r_{M_i} - r_{\text{Ce}} - 0.25r_{\text{O}} + 0.25r_{\text{V}}) m_i + \frac{4}{\sqrt{3}} \times (r_{\text{Ce}} + r_{\text{O}}) \right] \quad (1)$$

$$a = 5.413 + \sum_i \left[0.22(r_{M_i} - r_{\text{Ce}}) + 0.0015\Delta Z_i \right] m_i \quad (2)$$

where r_M , r_{Ce} , r_{O} , and r_{V} are the ionic radii of dopant, cerium, oxygen, and oxygen vacancy, respectively; ΔZ — charge differences between dopant and cerium cations; m — mole percent of the dopant. As can be seen, the eq. 1 is poor described the lattice parameter dependence, but eq. 2 is more suitable for this behavior. Unfortunately, for Cu-Mn-Zr-Ce-O solid solution cell parameter is not correlated with any equation, so the contribution of surface lattice relaxations to the variations of the lattice parameters cannot be excluded. The lattice parameter of sample 6 is higher than pure ceria (sample 0, [10]), because in according to a full height approximation of the spectrum the copper oxides can be probably found in the form of amorphous state, but is less than bulk ceria lattice parameter in eq. 2 (5.413 Å). Nevertheless, it is known that the preparing of homogeneous solid solutions gives the better textural property, thermal stability, catalytic properties and others compared to domain- or phase-segregated nonhomogeneous ones. SAED method (Fig. 2, inset) also confirmed the formation of the only phase of fluorite structure solid solution. According to TG-DSC, these solid solutions are stable up to 1400°C.

All samples have IV type adsorption curves with a hysteresis loop (Fig. 3), indicating the presence of mesopores in the systems. There was the increase of specific surface (Table 1) with increasing content of manganese or the decrease with adding zirconium. The hysteresis loops correspond to the type of H2. Pore size distributions present in Fig. 4: polymodal pore size distributions observed in the range of 2–25 nm for Cu-Mn-Ce-O systems and 2–40 nm for Cu-Mn-Zr-Ce-O. Apparently, individual or connected cylindrical and bottle-shaped pores may be present, formed between aggregates and agglomerates, and pores with predominantly diameter of 2–6 nm are formed by small-angle particle boundaries. No micropores (<2 nm, according to t-plot method) were observed in all samples, and no regularity in the change of Cu/Mn ratio was too. Unfortunately, this method did not allow creating narrow monomodal pore size distribution as in our earlier work [13, 14], but it may be done by using acetylacetone.

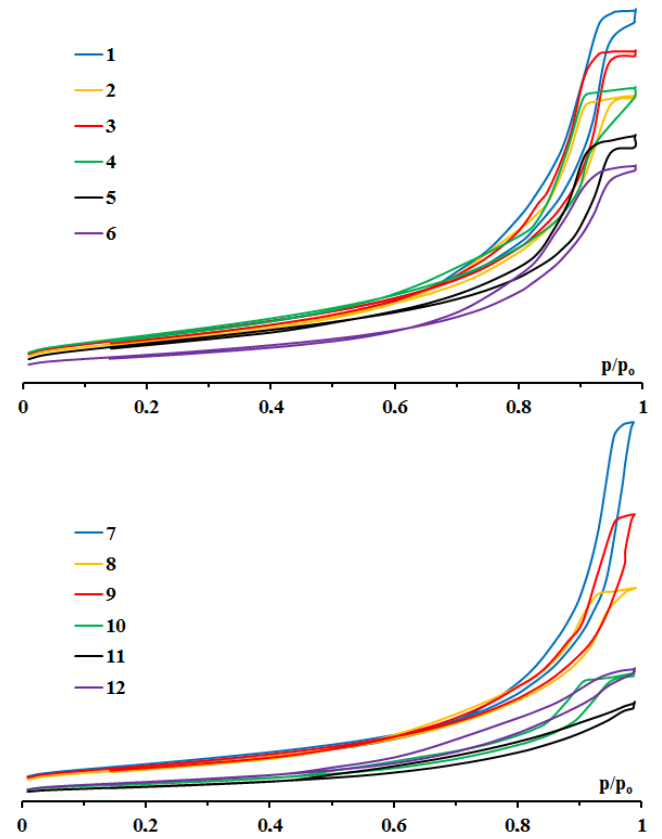


Fig. 3. (Color online) Adsorption-desorption isotherms (sample number corresponds to Table 1).

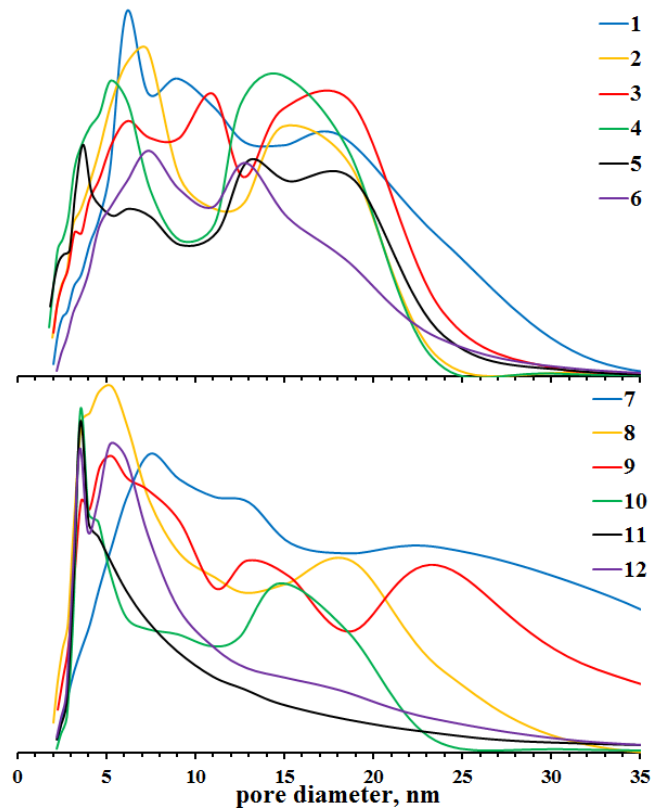


Fig. 4. (Color online) Pore size distributions.

4. Conclusions

Mesoporous Cu-Mn-Zr-Ce-O oxides with the crystallite size about 7–9 nm, not depending on the Cu/Mn ratio, were prepared via the co-precipitation method with sonication. Both Cu and Mn enter in ceria lattice to form solid solution. The semiempirical equation for ceria based solid solutions is clear described the lattice parameter dependence in Cu-Mn-Ce-O system, but in Cu-Mn-Zr-Ce-O system is not. Therefore, this method allowed creating such homogeneous solid solutions, giving the better properties for their application. These systems can be applied in catalysis as a support or in IT-SOFC as an electrolyte.

Acknowledgments. This research was supported by Russian Science Foundation (No. 17-73-10331). This work was partially conducted within the framework of budget project No. 007-00129-18-00.

References

1. Q. Liang, X. Wu, D. W., H. Xu. Catal. Today. 139, 113 (2008). DOI: 10.1016/j.cattod.2008.08.013
2. X. Zhou, M. Meng, Z. Sun, Q. Li, Z. Jiang. Chem. Eng. J. 174, 400 (2011). DOI: 10.1016/j.cej.2011.09.018
3. H. Lu, X. Kong, H. Huang, Y. Zhou, Y. Chen. J. Environ. Sci. 32, 102 (2015). DOI: 10.1016/j.jes.2014.11.015
4. H. Lu, Y. Zhou, H. Huang, B. Zhang, Y. Chen. J. Rare Earth. 29, 855 (2011). DOI: 10.1016/S1002-0721(10)60555-8
5. C. He, Y. Yu, J. Shi, Q. Shen, J. Chen, H. Liu. Mater. Chem. Phys. 157, 87 (2015). DOI: 10.1016/j.matchemphys.2015.03.020
6. D. V. Pinjari, A. B. Pandit. Ultra Sonochem. 18, 1118 (2011). DOI: 10.1016/j.ultsonch.2011.01.008
7. K. Singh, R. Kumar, A. Chowdhury. Ultra Sonochem. 36, 182 (2017). DOI: 10.1016/j.ultsonch.2016.11.030
8. A. Aranda, E. Aylón, B. Solsona, R. Murillo, A. M. Mastral, D. R. Sellick, S. Agouram, T. García, S. H. Taylor. Chem. Comm. 48, 4704 (2012). DOI: 10.1039/C2CC31206A
9. Ch. Y. Kang, H. Kusaba, H. Yahiro, K. Sasaki, Y. Teraoka. Solid State Ionics. 177, 1799 (2006). DOI: 10.1016/j.ssi.2006.04.016
10. I. V. Zagaynov, A. V. Vorobiev, S. V. Kutsev. Mater. Lett. 139, 237 (2015). DOI: 10.1016/j.matlet.2014.10.096
11. S. J. Hong, A. V. Virkar. J. Am. Ceram. Soc. 78, 433 (1995). DOI: 10.1111/j.1151-2916.1995.tb08820.x
12. D.-J. Kim. J. Am. Ceram. Soc. 72, 1415 (1989). DOI: 10.1111/j.1151-2916.1989.tb07663.x
13. I. V. Zagaynov, A. A. Konovalov. J. Porous Mater. 24, 1247 (2017). DOI: 10.1007/s10934-017-0365-6
14. I. V. Zagaynov. Appl. Nanosci. 7, 871 (2017). DOI: 10.1007/s13204-017-0625-4